Low Concentrations of Silver Nanoparticles and Silver Ions Perturb Antioxidant Defense System and Nitrogen Metabolism in N_2-Fixing Cyanobacteria

Min Huang[§], Arturo A. Keller[ζ], Xiaomi Wang[ξ], Liyan Tian[§], Bing Wu[§], Rong Ji[§], Lijuan Zhao[§]*

[§]State Key Laboratory of Pollution Control and Resource Reuse, School of Environment, Nanjing University, Nanjing 210023, China

ζBren School of Environmental Science & Management and Center for Environmental Implications of Nanotechnology, University of California, Santa Barbara, California 93106, United States

ξKey Laboratory of Soil Environment and Pollution Remediation, Institute of Soil Science, Chinese Academy of Sciences, Nanjing 210008, China

**Corresponding author*. Tel: +86 025-8968 0581; fax: +86 025-8968 0581.
Email address: ljzhao@nju.edu.cn

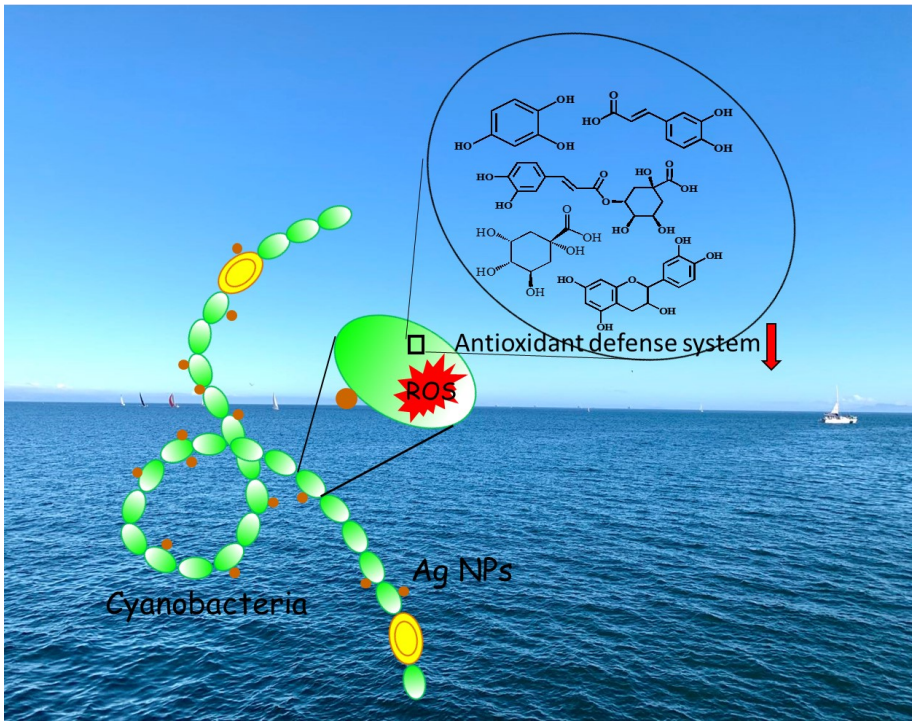

TOC

ABSTRACT

Although toxic effects of silver nanoparticles (AgNPs) on aquatic organisms have been extensively reported, the response of nitrogen-fixation cyanobacteria to AgNPs/Ag^+ under environmental relevant concentrations are largely unknown. Here, cyanobacteria were exposed to different concentrations of AgNPs (0.01, 0.1 and 1 mg/L) or Ag^+ (0.1, 1 and 10 μg/L) for 96 h. The impacts of AgNPs and Ag^+ on photosynthesis and N_2-fixing in cyanobacteria (*Nostoc sphaeroides*) were evaluated. In addition, gas chromatography-mass spectrometry (GC-MS) based metabolomics was employed to give an instantaneous snapshot of the physiological status of the cells under AgNPs/Ag^+ exposure. Exposure to high doses of AgNPs (1 mg/L) or Ag^+ (10 μg/L) caused growth inhibition, reactive oxygen species (ROS) overproduction, malondialdehyde (MDA) accumulation, and decreased N_2-fixing. In contrast, low doses of AgNPs (0.01, 0.1 mg/L) and Ag^+ (0.1 and 1 μg/L) did not induce observable responses. However, metabolomics revealed that metabolic reprogramming occurred even at low concentrations of AgNPs and Ag^+ exposure. Levels of a number of antioxidant defense related metabolites, especially phenolic acid and polyphenols (gallic acid, resveratrol, isochlorogenic acid, chlorogenic acid, cinnamic acid, 3-hydroxybenzoic acid, epicatechin, catechin, ferulic acid), were significantly decreased in response to AgNPs or Ag^+. Meanwhile, the levels of many amino acids and nitrogen-containing metabolites were significantly increased. This indicates that AgNPs and Ag^+ can disrupt the antioxidant defense system and disturb nitrogen metabolism even at low dose exposure. Metabolomics were shown to be a powerful tool to detect "invisible" changes, not observable by typical phenotypic based endpoint.

INTRODUCTION

The deployment of nanotechnology has resulted in increasing releases of various engineered nanoparticles (ENPs) into the environment annually. Silver nanoparticles (AgNPs) are by far the most commercialized ENPs in the market due to their excellent antibacterial capacities,[1] and the release and accumulation of AgNPs are expected to increase rapidly. Recently a few of groups investigated the environmental concentrations of AgNPs in water bodies. Based on these reports, the predicted and observed Ag concentrations in the effluent of wastewater treatment plant (WWTP) and surface water in Switzerland, [2] Swiss,[3] and U.S. [4, 5] are in a range of 0.04~0.2 μg/L. Due to inadequate elimination of AgNPs by WWTPs, aquatic ecosystem will be a main sink for AgNPs. [6, 7]

Understanding the interaction between AgNPs and aquatic organisms, such as algae, cyanobacteria and fish, is crucial for their environmental assessment. However, the current challenge in studying the toxicological effects of NPs on aquatic organisms is that high exposure doses would generate observable responses, but the real environmental risk can be compromised or mis-represented by the consideration of unrealistic exposure doses.[8] On the other hand, under low exposure doses, the toxic effects are difficult to detect by measuring typical phenotypic based endpoints, e.g. growth, photosynthesis, lipid peroxidation.[9] New tools and endpoints are necessary to detect the traditional "invisible" changes in organisms exposed to NPs at environmental relevant concentrations. Omics are sensitive and powerful tools which can capture molecular changes in organisms. Thus, omics-based endpoints may enable the observation of molecular changes that provide an early warning on metabolic profile alterations.[10] Among all the omics techniques, metabolomics provides a direct and instantaneous

snapshot of the physiological state of the cell, without considering the genetic changes.[11] Under environmental stress conditions, reprogramming of metabolome may occur in the cell, leading to a targeted metabolic strategy to cope with stress.

Cyanobacteria are ecologically important primary producers in freshwater and marine environments. The photosynthetic impacts of AgNPs on a number of cyanobacteria species (*Synechococcus leopoliensis*[12], *Synechococcus sp.*[13] and *microcystis aeruginosa*[14]) have been investigated. However, certain cyanobacteria species can perform nitrogen-fixation and oxygenic photosynthesis simultaneously.[15, 16] These nitrogen-fixation cyanobacteria play important roles in both carbon (C) and nitrogen (N) cycling in aquatic ecosystems. Cyanobacteria can also play an important role in supplying nitrogen to non-legume plants, such as maize and rice. Therefore, understanding the impacts of AgNPs on cyanobacteria, especially N_2-fixation and nitrogen metabolism, is of great importance, but few studies have addressed these issues.

The goals of this study were to investigate the response of N_2-fixing cyanobacteria (*Nostoc sphaeroides*) to AgNPs at low concentrations of exposure. Two important biological functions, photosynthesis and N_2-fixing, were evaluated simultaneously. Since AgNPs are known to induce the overproduction of reactive oxygen species (ROS), ROS homeostasis and antioxidant defense system were also evaluated. In addition, by using gas chromatography-mass spectrometry (GC-MS) based metabolomics, we sought to detect "invisible" metabolic changes at low exposure doses, which may help to understand the mechanisms and underlying processes governing the toxicity of AgNPs to cyanobacteria. The findings of this work will contribute to a thorough, deep and comprehensive understanding of the response of cyanobacteria to AgNPs.

EXPERIMENTAL SECTION

AgNPs Characterization. AgNPs were purchased from Pantian nano Material Co., Ltd. (Shanghai, China). The size, shape, and morphology of AgNPs were observed by transmission electron microscope (TEM) (JEM-200CX, JEOL, Japan). A typical TEM image reveals that the AgNPs are roughly spherical in shape with sizes in the range of 19.9~36.9 nm (**Figure S1**), with an average of 30.87 nm. The hydrodynamic diameter of AgNPs in ultrapure water, at 100 mg/L, was 134.7 ± 1.38 nm, with a ζ potential of 9.95 ± 0.76 mV, measured via dynamic light scattering (Zetasizer Nano ZS, Malvern). An AgNPs stock suspension was prepared by adding 1 mg of Ag NPs into 100 mL of DI water and sonicated (KH-100DB, Hechuang Utrasonic, Jiangsu, China) at 45 kHz for 30 min to obtain a well dispersed suspension.

Cyanobacteria Culture and AgNPs Exposure. *Nostoc sphaeroides* cyanobacteria were obtained from the Institute of Wuhan Hydrobiology, Chinese Academy of Sciences. The growth medium used for routine culture of *Nostoc* and for AgNPs exposure experiments was BG11-N (BG11 without nitrogen, composition in **Table S1**). *Nostoc* were cultured at 25 ± 1 °C with a 12h/12h light/dark cycle with light intensity of 36 μmol photons m^{-2} s^{-1}. Cell densities were measured using optical density at 680 nm (OD 680) with a microplate spectrophotometer (Synergy H4 Hybrid Reader, Biotek, America).

Seven treatments were established, including control (no Ag^+ or AgNPs), 0.01, 0.1, and 1 mg/L AgNPs; 0.1, 1, and 10 μg/L Ag^+. Previous studies[17, 18] and our preliminary experiments showed that approximately 1% of Ag^+ were released from AgNPs over 96 h. These AgNPs and Ag ion concentrations covered a wide range of possible environmentally relevant levels. Each treatment had 4 replicates. The AgNPs stock

solutions were prepared immediately prior to exposure experiments. The algal cells were mixed with AgNPs or $AgNO_3$ suspensions in 250 mL sterilized flasks and placed in shakers (100 rpm, 25 ± 1 °C) for up to 96 h.

Morphology of Cyanobacteria Cells. The morphology of cyanobacteria cells and the distribution of AgNPs on the cell surface were observed using scanning electron microscope (SEM) (FEI Quanta 250 FEG) equipped with an energy dispersive X-ray spectrometry (EDS) (Oxford Aztec X-ManN80). Briefly, the samples were fixed in 2.5% glutaraldehyde, dehydrated in gradient concentrations of ethanol, coated with a layer of gold, and then the images were observed and analyzed for Ag distribution using SEM and EDS.[19]

Cell Density and Chlorophyll Content. The cell density of *Nostoc sphaeroides* was monitored using a multi-mode microplate reader (Synergy H4 Hybrid Reader, Biotek, America) at an absorption wavelength of 680 nm (OD 680). The chlorophyll α measurement was performed according to Sigalat and de Kouchkowski.[20]

Nitrogenase Activity and Total Nitrogen. Nitrogen fixation activity is usually measured by the $^{15}N_2$ stable isotope method or by Acetylene-Reduction Assay (ARA).[21] It is believed that $^{15}N_2$ is the most reliable method as this method directly measures N fixation. However, $^{15}N_2$ is costly and requires highly controlled conditions, while the ARA assay is fast and less expensive. Therefore, the nitrogen fixation activities were measured according to ARA protocol described by Wang et al.[22] The principle of the ARA assay is that the nitrogenase enzyme produces ethylene (C_2H_4) in the presence of acetylene (C_2H_2), so the production of C_2H_4 reflects nitrogenase activity.[21] Specifically, NP-cyanobacteria suspensions were incubated with 10% acetylene in 10 ml serum bottles at 25 °C for 4 h.

After incubation, the amount of ethylene in the gas phase was quantified using an Agilent 6850 gas chromatograph equipped with a hydrogen flame ionization detector and a HP-PLOT U column (30 m × 0.32 mm, 10 μm) (Agilent Technologies, La Jolla, CA, U.S.A.). The injection and detector temperatures were 120 °C and 220 °C, respectively. The column was held at 50 °C for 8 min. The amount of ethylene produced was assessed by measuring the height of the ethylene peak on the chromatogram relative to the length of the reaction. Dilution of pure ethylene was employed to create five-point standard calibration curves ($y = 15.668x + 48.094$, $R^2 = 0.998$). The detection limit for ethylene was ~2 nmol L^{-1}. Ethylene production occurred linearly over the assay period.

The total nitrogen in cyanobacteria was determined according to the method reported by Studt et al.[23] In the method, the alkaline persulfate reaction oxidizes all nitrogen present in cyanobacteria cells to nitrate, then nitrate reductase is used to catalyze the reduction of nitrate to nitrite in the presence of NADH (nicotinamide adenine dinucleotide). Griess reagents are added to react with nitrate and produce a pink color. The absorbance was measured at 540 nm using a multi-mode microplate reader (Synergy H4 Hybrid Reader, Biotek, America).

ROS Levels and Lipid Peroxidation in Cyanobacteria Cells. ROS production in cyanobacterial cells were quantified using 2,7-dichlorofluorescein diacetate (H_2DCFDA) as a fluorescence probe.[24] The *Nostoc* cells (1 mL) were incubated with H_2DCFDA (10 μmol/L) at 25 °C for 30 min. The cells were then washed 3 times with phosphate buffer saline (PBS) at 0.01 μmol/L and re-suspended in 200 μL PBS. The fluorescence of the molecular probes was detected using a microplate reader (Synergy H4 Hybrid Reader,

Biotek, America), with an excitation wavelength of 488 nm and an emission wavelength of 525 nm. Three replicates were performed for each measurement.

The membrane integrity of mesophyll protoplasts was evaluated by measuring MDA content, which is the final product of lipid peroxidation. The MDA content was measured by the Thiobarbituric Acid Reactive Substances (TBARS) assay.[25] Specifically, 1 ml of mesophyll protoplast-NPs (2×10^6) was mixed with 0.3 mL of 0.1% trichloroacetic acid; the mixture was then centrifuged at 10619 × g for 15 min. A 0.2 mL aliquot of the supernatant was mixed with 0.8 mL of 0.5% thiobarbituric acid. After this the mixture was heated in a water bath at 95 °C for 30 min. After cooling, the UV absorbance was measured at 450, 532 and 600 nm via a microplate reader (Varioskan LUX, Thermo Fisher Scientific, Vantaa, Finland). Lipid peroxidation was expressed as μmol of MDA equivalent per gram of mesophyll protoplasts.

GC-MS Based Cyanobacteria Metabolomics. After exposure to different concentrations of AgNPs or Ag^+ for 96 h, cyanobacteria cells (15 ml) were collected by centrifugation for metabolome analysis. The cell pellets were then washed 3 times with PBS buffer. Subsequently, the washed cell pellets were immediately frozen in liquid nitrogen for 20 s for complete metabolic inactivation.[26] The frozen samples were stored at -80 °C. The metabolites were extracted from deep-frozen cells using 80% methanol containing a defined amount of the internal standard 2-chloro-l-phenylalanine (0.3 mg/mL). Chloroform and water were added to separate polar and lipophilic metabolites by phase separation. The phase containing the polar metabolites was dried by vacuum-drying. The extracted compounds were derivatized using methoxylamine hydrochloride and subsequent N,O-bis(trimethylsilyl) trifluoroacetamide (BSTFA). An Agilent 7890B

gas chromatograph coupled to an Agilent 5977A mass selective detector (Santa Clara, CA, USA), with a DB-5MS fused-silica capillary column (30 m × 0.25 mm internal diameter with 0.25 μm film) (Agilent J & W Scientific, Folsom, CA, USA), was used to run the samples. Quantification was reported as peak height using unique ion as default. Metabolites were unambiguously assigned by the BinBase identifier numbers using retention index and mass spectrum as the two most important identification criteria.

Metabolomics Data Analysis. For GC-MS data, a supervised partial least-squares discriminant analysis (PLS-DA) clustering method was run via online resources (http://www.metaboanalyst.ca/).[27] Before PLS-DA, the data normalization (normalization by sum) was performed for general-purpose adjustment based on the differences among samples, and data transformation (log transformation) was conducted to make individual features more comparable. Variable Importance in Projection (VIP) is the weighted sum of the squares of the PLS-DA analysis, which indicates the importance of a variable to the entire model.[28] A variable with a VIP greater than 1 is regarded as responsible for separation, defined as a discriminating metabolite in this study.[29] Biological pathway analysis was performed based on the GC-MS data using MetaboAnalyst 2.0.[30] The impact value threshold calculated for pathway identification was set at 0.1.[29]

Statistical Analysis. Each treatment was conducted in four replicates. For physiological and biochemical assays, the experimental data are represented as mean ± standard deviation. A one-way ANOVA test was performed followed by Tukey-HSD test using the statistical package SPSS 22.0 (SPSS, Chicago, IL).

RESULTS AND DISCUSSION

***Nostoc* Cyanobacteria Cell Morphology and AgNPs Localization.** Adsorption and direct contact of NPs with aquatic microorganisms are a prerequisite for toxicity.[31] SEM imaging was used to provide visual identification of the interaction between AgNPs and cyanobacteria. As shown in the SEM images, cyanobacteria cells are arranged in bead-like chains (**Figure 1**). A typical single cell has a length of 3.36 μm and width of 2.22 μm. The adsorption of NPs onto surfaces of aquatic organisms is governed by multiple factors, such as the physicochemical properties of the NPs and biological substrate (e.g., cell type, cell membrane, and the pathways of cellular processing).[32, 33] The forces involved in adsorption of NPs on cells include van der Waals forces, hydrophobic forces, electrostatic attraction and specific chemical interactions.[34] The positively charged AgNPs (+9.95 mV) likely adhere on the cyanobacteria cell surface through electrostatic attraction. Another finding is that the shape, integrity, and surface morphology of the cells were unchanged by exposure to AgNPs at 0.1 mg/L. It has been reported that the close particle attachment to the algal cell can result in NP internalization.[35]

Effect of AgNPs and Ag^+ on the Growth of Cyanobacteria. After the exposure to different concentrations of AgNPs and Ag^+ for 96 h, cyanobacteria biomass was evaluated via determination of Optical Density at 680 nm (OD 680). Results showed that *Nostoc sphaeroides* biomass was unchanged upon exposure to low and medium concentrations of AgNPs (0.01 and 0.1 mg/L) and Ag^+ (0.1 and 1 μg/L) (**Figure 2 A and B**). However, high concentrations of AgNPs and Ag^+ significantly (p<0.05) decreased cyanobacteria biomass by 25.8% and 10.7%, respectively, compared to the control (**Figure 2 A and B**). Similarly, chlorophyll content was unchanged upon exposure to low

and medium concentrations of AgNPs and Ag^+, while high concentration of AgNPs and Ag^+ significantly (p<0.01) decreased chlorophyll content by 32.3% and 18.3%, respectively, compared to the control (**Figure 2 C and D**). In addition, a marked visible discoloration in cyanobacteria exposed to high concentration of AgNPs or Ag^+ can be observed (see photographic images of cyanobacteria in **Figure 2 E and F**). These data indicate that AgNPs and Ag^+ at the high doses partially inhibited cyanobacteria growth and photosynthesis. These results are not surprising, and consistent with previous studies.[36, 37] AgNPs exposed to AgNPs or Ag^+ can result in the formation of oxygen free radicals, which will induce oxidative stress and lead to the inhibited cyanobacteria growth. [38]

Cyanobacteria Nitrogen Fixation. Since photosynthesis is the principal energy source of adenosine triphosphate (ATP) for driving nitrogen fixation,[39] we evaluated whether nitrogen fixation activities were impacted by exposure to AgNPs or Ag^+. Nitrogenase activity, reflected by C_2H_4 production, is shown in **Figures 3 A and B**. Nitrogen fixation activity was unchanged upon exposure to low and medium concentrations of AgNPs and Ag^+, but was significantly (p<0.05) decreased at high concentrations of AgNPs (94.0%) and Ag^+ (31.0%). Heterocysts are considered the sites of nitrogen fixation by the nitrogenase enzyme. Compared with vegetative cells, heterocyst cells have thick walled modified cells, which help to protect the enzyme nitrogenase from oxygen attack. The decreased N_2-fixating activity may come from either direct disruption of heterocyst's cell membrane, or indirectly influenced by the compromised photosynthesis of vegetative cells. To verify if AgNPs and Ag^+ decreased N_2-fixing, the total nitrogen content was determined in cyanobacteria after 96 h of exposure. A high concentration of AgNPs and

Ag^+ significantly (p<0.05) decreased total N content by 23.5% and 6.2%, respectively in *Nostoc* (**Figure 3 C and D**), which is consistent with the nitrogen fixation activity findings.

Antioxidant System. It has been recognized that AgNPs trigger the overproduction of ROS, which in turn leads to cytotoxicity. After exposure to different concentrations of AgNPs for 96 h, ROS production in cyanobacteria cells was increased generally in a dose-dependent manner (**Figure 4 A**). Medium (0.1 mg/L) and high dose (1 mg/L) of AgNPs exposure significantly (p<0.05) increased ROS content in cyanobacteria cells (**Figure 4 A**). Ag^+ also induced dose-dependent ROS increase in cyanobacteria cells (**Figure 4 B**). The high dose of Ag^+ significantly ($p\leq0.05$) increased ROS by 100%, compared to the control (**Figure 4 B**). These findings are consistent with a previous report that AgNPs and Ag^+ induced overproduction of ROS in algae cells (*Chattonella marina*).[40] He et al. also attribute the toxicity of AgNPs to the triggered overproduction of reactive oxygen species.[40]

Lipid membranes are among the most vulnerable cellular components to oxidative stress.[41] MDA, the byproduct of lipid peroxidation, was employed to evaluate whether the overproduced ROS damaged the cell membranes. Results showed that low and medium concentrations of AgNPs and Ag^+ did not change MDA content in *Nostoc* (**Figure 4 C and D**). However, MDA content was significantly increased (p<0.01, t-test) upon exposure to high dose of AgNPs (**Figure 4 C**) and Ag^+ (**Figure 4 D**). This indicates that the membrane is the target of ROS-induced attack by AgNPs . Meanwhile, the increased ROS and MDA can explain the growth inhibition after exposure to high dose of AgNPs or Ag^+.

Cell Metabolomics in Response to AgNPs and Ag^+. The above phenotypic and biochemical based endpoints reveal that only the higher dose of AgNPs (1 mg/L) or Ag^+ (10 μg/L) induced growth inhibition and reduction in nitrogen fixation within 96 h. Using a nontargeted GC-MS based metabolomics, we sought to determine whether metabolomics could reveal some "invisible" changes in cyanobacteria cells exposed to low concentrations of AgNPs or Ag^+, by identifying and quantifying changes in metabolite levels. A total of 193 metabolites were identified and semi-quantified. A multivariate analysis, partial least squares-discriminant analysis (PLS-DA), was conducted to obtain a global view of how the metabolite profile changed. The score plot of PLS-DA model show that AgNPs groups are separated from the control group generally in a dose-dependent manner along PC1 (**Figure 5 A**). Similarly, all Ag^+ groups were clearly separated from the control in a dose-dependent way (**Figure 5 B**), as reflected by the score plot. These data indicate that even low and medium concentrations of AgNPs (0.01 and 0.1 mg/L) and Ag^+ (0.1 and 1 μg/L) induced global metabolic reprogramming of intermediates in cyanobacteria, in other words, even low concentration of AgNPs and Ag^+ disrupted the normal metabolism of cyanobacteria, although there is no observable response at phenotypic and biochemical level.

To screen out metabolites which differed in concentration between the control and AgNPs/Ag^+ exposed groups, univariate analysis (ANOVA and *t*-test) was performed. Levels of 48 and 102 metabolites were found significantly changed upon exposure to AgNPs and Ag^+ (see Venn diagram in **Figure 5 C**), respectively, while 39 metabolites overlapped (**Figure 5 C** and **Table S2**). It is noteworthy that most of the overlapped metabolites are involved in ROS quenching and antioxidant defense. For example, some

phenolic acids and polyphenols, including gallic acid, resveratrol, isochlorogenic acid, chlorogenic acid, cinnamic acid, hydroquinone, 3-hydroxybenzoic acid, 1,2,3-trihydroxybenzene, quinic acid, epicatechin, catechin, ferulic acid, and 1,3,5-benzetriol, are decreased in a dose-dependent manner with AgNPs and Ag^+ (see boxplot in **Figure 6**). These phenolic acids are produced in plants via shikimic acid through shikimate-phenylpropanoid biosynthesis.[42] Interestingly, two aromatic amino acids (L-tyrosine and phenylalanine), which are precursors for phenolics biosynthesis in the shikimate-phenylpropanoid pathway, increased in a dose-dependent manner after exposure to AgNPs (**Figure S2**). The consumption of phenolic acids and the upregulation of their up-stream precursors indicates that biological pathways for producing antioxidants were activated to defend against overproduced ROS due to exposure to AgNPs or Ag^+.

In addition to phenolic acids or phenolics, more significantly changes in levels of metabolites associated with antioxidant defense were observed. For example, AgNPs and Ag^+ caused a significant decrease of oxalic acid (42%~64%) in a dose-dependent manner as compared with the control (**Figure 7**). It has been reported that oxalic acids are able to inhibit the production of H_2O_2, thus can modulate the oxidative burst of the plant.[43] The down-regulation of oxalic acid may indicate a stress defense mechanism in cyanobacteria cell in response to AgNPs. Dehydroascorbic acid (DHA), which is an oxidized form of ascorbic acid (vitamin C), decreased in a dose-dependent manner with AgNP and Ag^+ exposure (**Figure S3**). DHA is the product of an important antioxidant-associated pathway (ascorbate and aldarate metabolism), acting as a cellular protector against oxidative stress.[44] The consumption of these antioxidant metabolites possibly quenched the overproduction of ROS induced by Ag^+, and prevented the damage to important

cellular components. The down-regulation of so many antioxidant related compounds indicate that the antioxidant defense system was activated by AgNPs and Ag^+, even at a low exposure dose. We measured total antioxidant capacity (TAC) in cyanobacteria cells and found that high concentration of AgNPs (1 mg/L) and Ag^+ (10 μg/L) significantly (p<0.05) reduced TAC by 15.8% and 10.6, respectively (**Figure S4 A and B**).

Only one antioxidant related compound, glutathione (GSH), was observed to significantly increase after exposure to either AgNPs ot Ag^+ (**Figure S5**). GSH not only acts as a signaling molecule, but also plays an important role in protecting macromolecules against attack by eliminating free radicals, which are formed as a consequence of oxidative stress.[45] These metabolites might be the second line of antioxidant defense, compared to phenolics. Taken together, the above finding indicates that even low concentrations of AgNPs and Ag^+ activated the antioxidant defense system of cyanobacteria, at levels below those reflected by determination of ROS and MDA contents. This indicates that MDA, a well-known lipid peroxidation biomarker, does not necessarily provide an early and sensitive warning that antioxidant system has been disrupted. Since the equilibrium between ROS generation and consumption was broken, the growth and development of cyanobacteria will be compromised leading even to death after a long-term exposure, although low and medium concentrations of AgNPs and Ag^+ did not induce growth inhibition within 96 h.

Changed N-containing Compounds and Fatty Acids by AgNPs and Ag^+. As discussed before, the N_2-fixing of cyanobacteria was negatively impacted by AgNPs and Ag^+ exposure at high concentration. Therefore, it is expected that the nitrogen-containing metabolites will be decreased by AgNPs exposure accordingly. Unexpectedly, a number

of N-containing compounds, such as allantoic acid, methoxyamine, hippuric acid, creatinine, butylamine, 2-ketoadipic acid, N-acetylornithine, N-acetylputrescine were significantly increased in a dose-dependent manner with AgNPs and Ag^+ exposure (**Figure S6**). The up-regulation of these compounds may indicate that the catabolism of protein/amino acids was accelerated in order to compensate for the decreased nitrogen pool. Among the N-containing compounds, 2-ketoadipic acid is an intermediate in l-tryptophan and l-lysine catabolism. Allantoic acid is intermediate in the purine degradation pathway.

Another noteworthy change is that some saturated fatty acids (palmitelaidic acid, palmitic acid, and lignoceric acid) increase after exposure to low and medium concentrations of AgNPs and Ag^+, but decreased under high dose (**Figure S7**). The up-regulation of saturated fatty acids may indicate a strategy of cyanobacteria to protect the cell from ROS attack by altering the composition of the plasma cell membrane and changing the permeability of the cell membrane. When ROS was over-produced under high AgNPs/Ag^+ exposure, the cell membrane was damaged and the level of these fatty acids decreased.

Ag^+ Specific Metabolic Changes. The above discussion addressed metabolic changes that were common to AgNPs and Ag^+, such as decreased antioxidant compounds, increased nitrogen-containing compounds, and perturbed unsaturated fatty acids. The similarities in the metabolic reprogramming pattern suggest that part of the responses in cyanobacteria induced by AgNPs are due to the dissolved Ag ions. However, it cannot be neglected that Ag^+ induced a much stronger metabolic response compared to AgNPs. As can be seen in **Figure S8**, levels of additional antioxidant related metabolites (pelargonic

acid, protocatechoic acid, and alpha tocopherol, 1,2,4-benzenetriol) were decreased by Ag^+, compared to AgNPs (**Figure 6**). Furthermore, unlike AgNPs exposure which gradually decreased antioxidants with increasing AgNPs exposure concentration (see box plot in **Figure 6**), Ag^+ even at the lowest dose induced a marked decrease in antioxidant levels (**Figure S8**). This indicates that Ag^+ directly induced more pronounced negative effects on the antioxidant defense system. Taylor et al.[12] also found that ionic silver had more negative effects, compared to AgNPs, on the toxic stress endpoints. This may reflect the slow release dynamics of Ag^+ from AgNPs, compared to Ag^+ from $AgNO_3$ which is almost immediately available.

Additionally, levels of a number of metabolites, which were unchanged by exposure to AgNPs, were increased by Ag^+ treatment, such as ethylamine, nicotinic acid, inositol-4-monophosphate, urea, malic acid, serine, glycine, norvaline, thymine, lysine, glutamic acid, aspartic acid, threonine, ribose, D-fructose-6-phosphate, glucose-6-phosphate. Again, this indicates that Ag^+ induced a stronger response to the oxidative stress and more pronounced metabolic reprogramming, compared to AgNPs. Possibly, the up-regulation of these compounds is the strategy cyanobacteria employed to cope with the disrupted ROS homeostasis. In **Figure S9**, six amino acids (glycine, serine, L-threonine, L-aspartic acid, glutamic acid, thymine), one organic acid (malic acid), and two sugars (D-fructose-6-phosphate, glucose-6-phosphate) share very similar metabolic change patterns under Ag^+ treatment. Levels of these metabolites increased in a dose-dependent manner from control to low and medium dose, but then either did not increase or even declined at high concentration of Ag^+ exposure. We speculate that cyanobacteria cells actively reprogram the metabolome to cope with the stress before Ag^+ reach the threshold.

The changes of these carbohydrates and amino acids are indicative of perturbations to carbon and nitrogen metabolism.

Metabolic pathway analysis reveals that AgNPs at low concentration (0.01 mg/L) did not induce any pathway perturbation (**Table S3**), while even the lowest dose of Ag^+ (0.1 μg/L) induced perturbation of 9 biological pathways, including beta-alanine metabolism; glyoxylate and dicarboxylate metabolism; arginine biosynthesis; cysteine and methionine metabolism; pantothenate and co-enzyme A biosynthesis; glycine, serine and threonine metabolism; arginine and proline metabolism; isoquinoline alkaloid biosynthesis; and tyrosine metabolism (**Table S3**). Medium and high concentrations of Ag^+ induced perturbations in 14 and 21 biological pathways, respectively (**Table S3**). In contrast, medium and high concentrations of AgNPs induced only 10 and 12 metabolic pathway perturbations. Therefore, pathway analysis confirmed that Ag^+ induced more pronounced metabolic changes compared to AgNPs. Most of the pathways perturbed by AgNPs and Ag^+ were related to nitrogen metabolism, as indicated by the nitrogen assays. Carbon metabolism is linked to the incomplete tricarboxylic acid cycle (TCA cycle) in cyanobacteria cells; perturbations to a number of carbon related metabolic pathways were observed, such as glyoxylate and dicarboxylate metabolism, starch and sucrose metabolism. Taken together, although low concentrations of AgNPs and Ag^+ did not impact N_2 fixation, carbon and nitrogen metabolism were perturbed.

Environmental Implication. In this study, we systematically investigated the impact of AgNPs on a N_2-fixing cyanobacteria (*Nostoc sphaeroides*) during short term exposure (96 h); these cyanobacteria are important components of many ecosystems. In addition to considering typical phenotypic and biochemical based endpoints (OD 680, chlorophyll,

ROS, MDA) to evaluate the impact of AgNPs on cyanobacteria, we also evaluated , the metabolic responses of *Nostoc* cyanobacteria to AgNPs and Ag^+ via GC-MS based metabolomics. While only high doses of AgNPs and Ag^+ induced physiological responses (growth inhibition, overproduction of ROS, increased MDA, and decreased N_2-fixation), indicating the imbalance of ROS homeostasis and oxidative stress, metabolomics revealed that even low doses of AgNPs and Ag^+ induced metabolite profile alterations in *Nostoc sphaeroides*. Levels of a number of antioxidant related metabolites, especially phenolics, were marketable decreased upon exposure to either AgNPs or Ag^+, even at low dose, indicating a perturbed antioxidant defense system. AgNPs also induced the up-regulation of N-containing compounds, indicating perturbations to nitrogen metabolism. Since cyanobacteria play an important role in C and N cycling in ecosystem, the perturbed antioxidant system and nitrogen metabolism by AgNPs and Ag^+ will indirectly influence C and N cycling in aquatic or terrestrial ecosystem. In this study, the lowest concentration of Ag^+ (0.1 μg/L) evaluated falls within the range of observed environmental concentrations (0.04~0.2 μg/L). We demonstrate that even at such a low dose, Ag^+ can perturb the metabolism in cyanobacteria, disrupting the antioxidant defense system. Small molecules are markedly regulated by upstream gene expression and transcript formation; thus, changes in gene expression must have occurred even at low doses of Ag^+. Metabolomics can serve to detect these “invisible” changes. The physiological changes which typical endpoints cannot detected may be captured by metabolomics.

ACKNOWLEDGMENTS

This work was funded by National Natural Science Foundation of China under 31861133003 and 21876081. A. Keller was funded by United States National Science Foundation 1901515. Any opinions, finding, and conclusions or recommendations expressed in this material are those of authors and do not necessarily reflect the views of National Science Foundation of China or the United States National Science Foundation.

Supporting Information. Composition of BG11-N (**Table S1**); Metabolites significantly changed in cyanobacteria exposed to AgNPs or Ag^+ (**Table S2**); Perturbed metabolic pathways in cyanobacteria cells by AgNPs (0, 0.01, 0.1, 1 mg/L) and Ag^+ (0, 0.1, 1, 10 μg/L) exposure (**Table S3**); TEM image of AgNPs (**Figure S1**); Box plot of L-tyrosine and Phenylalanine levels in cyanobacteria cells (**Figure S2**); Box plot of Dehydroascorbic acid (DHA) levels in cyanobacteria cells (**Figure S3**); TAC of cyanobacteria cells (**Figure S4**); Box plot of glutathione (GSH) levels in cyanobacteria cells with AgNPs and Ag^+ exposure (**Figure S5**); Box plot of relative abundance of N-containing compounds in cyanobacteria cells with AgNPs and Ag^+ exposure (**Figure S6**); Box plot of saturated fatty acids in cyanobacteria cells with AgNPs and Ag^+ exposure (**Figure S7**); Box plot of antioxidant related metabolites exposed to Ag^+ (**Figure S8**); Box plot of 6 amino acids, 1 organic acids, and 2 sugars exposed to Ag^+ (**Figure S9**). This material is available as Supporting Information. This material is available free of charge via the Internet at http://pubs.acs.org.

REFERENCES

1. Flores-López, L. Z.; Espinoza-Gómez, H.; Somanathan, R., Silver nanoparticles: Electron transfer, reactive oxygen species, oxidative stress, beneficial and toxicological effects. Mini review. **2019,** *39* (1), 16-26.
2. Mueller, N. C.; Nowack, B., Exposure Modeling of Engineered Nanoparticles in the Environment. *Environmental Science & Technology* **2008,** *42* (12), 4447-4453.
3. Gottschalk, F.; Sonderer, T.; Scholz, R. W.; Nowack, B., Modeled Environmental Concentrations of Engineered Nanomaterials (TiO2, ZnO, Ag, CNT, Fullerenes) for Different Regions. *Environmental Science & Technology* **2009,** *43* (24), 9216-9222.
4. Mitrano, D. M.; Lesher, E. K.; Bednar, A.; Monserud, J.; Higgins, C. P.; Ranville, J. F., Detecting nanoparticulate silver using single-particle inductively coupled plasma–mass spectrometry. *Environmental Toxicology and Chemistry* **2012,** *31* (1), 115-121.
5. Cervantes-Avilés, P.; Huang, Y.; Keller, A. A., Incidence and persistence of silver nanoparticles throughout the wastewater treatment process. *Water Research* **2019,** *156*, 188-198.
6. Kaegi, R.; Voegelin, A.; Ort, C.; Sinnet, B.; Thalmann, B.; Krismer, J.; Hagendorfer, H.; Elumelu, M.; Mueller, E., Fate and transformation of silver nanoparticles in urban wastewater systems. *Water Research* **2013,** *47* (12), 3866-3877.
7. Lazareva, A.; Keller, A. A., Estimating Potential Life Cycle Releases of Engineered Nanomaterials from Wastewater Treatment Plants. *ACS Sustainable Chemistry & Engineering* **2014,** *2* (7), 1656-1665.
8. Liu, S.; Lu, Y.; Chen, W., Bridge knowledge gaps in environmental health and safety for sustainable development of nano-industries. *Nano Today* **2018,** *23*, 11-15.
9. Holden, P. A.; Gardea-Torresdey, J. L.; Klaessig, F.; Turco, R. F.; Mortimer, M.; Hund-Rinke, K.; Cohen Hubal, E. A.; Avery, D.; Barceló, D.; Behra, R.; Cohen, Y.; Deydier-Stephan, L.; Ferguson, P. L.; Fernandes, T. F.; Herr Harthorn, B.; Henderson, W. M.; Hoke, R. A.; Hristozov, D.; Johnston, J. M.; Kane, A. B.; Kapustka, L.; Keller, A. A.; Lenihan, H. S.; Lovell, W.; Murphy, C. J.; Nisbet, R. M.; Petersen, E. J.; Salinas, E. R.; Scheringer, M.; Sharma, M.; Speed, D. E.; Sultan, Y.; Westerhoff, P.; White, J. C.; Wiesner, M. R.; Wong, E. M.; Xing, B.; Steele Horan, M.; Godwin, H. A.; Nel, A. E., Considerations of Environmentally Relevant Test Conditions for Improved Evaluation of Ecological Hazards of Engineered Nanomaterials. *Environmental Science & Technology* **2016,** *50* (12), 6124-6145.
10. Buesen, R.; Chorley, B. N.; da Silva Lima, B.; Daston, G.; Deferme, L.; Ebbels, T.; Gant, T. W.; Goetz, A.; Greally, J.; Gribaldo, L.; Hackermüller, J.; Hubesch, B.; Jennen, D.; Johnson, K.; Kanno, J.; Kauffmann, H.-M.; Laffont, M.; McMullen, P.; Meehan, R.; Pemberton, M.; Perdichizzi, S.; Piersma, A. H.; Sauer, U. G.; Schmidt, K.; Seitz, H.; Sumida, K.; Tollefsen, K. E.; Tong, W.; Tralau, T.; van Ravenzwaay, B.; Weber, R. J. M.; Worth, A.; Yauk, C.; Poole, A., Applying 'omics

technologies in chemicals risk assessment: Report of an ECETOC workshop. *Regulatory Toxicology and Pharmacology* **2017,** *91*, S3-S13.
11. Kumar, R.; Bohra, A.; Pandey, A. K.; Pandey, M. K.; Kumar, A., Metabolomics for Plant Improvement: Status and Prospects. **2017,** *8* (1302).
12. Taylor, C.; Matzke, M.; Kroll, A.; Read, D. S.; Svendsen, C.; Crossley, A., Toxic interactions of different silver forms with freshwater green algae and cyanobacteria and their effects on mechanistic endpoints and the production of extracellular polymeric substances. *Environmental Science: Nano* **2016,** *3* (2), 396-408.
13. Burchardt, A. D.; Carvalho, R. N.; Valente, A.; Nativo, P.; Gilliland, D.; Garcìa, C. P.; Passarella, R.; Pedroni, V.; Rossi, F.; Lettieri, T., Effects of Silver Nanoparticles in Diatom Thalassiosira pseudonana and Cyanobacterium Synechococcus sp. *Environmental Science & Technology* **2012,** *46* (20), 11336-11344.
14. Qian, H.; Zhu, K.; Lu, H.; Lavoie, M.; Chen, S.; Zhou, Z.; Deng, Z.; Chen, J.; Fu, Z., Contrasting silver nanoparticle toxicity and detoxification strategies in Microcystis aeruginosa and Chlorella vulgaris: New insights from proteomic and physiological analyses. *Science of The Total Environment* **2016,** *572*, 1213-1221.
15. Singh, J. S.; Kumar, A.; Rai, A. N.; Singh, D. P., Cyanobacteria: A Precious Bio-resource in Agriculture, Ecosystem, and Environmental Sustainability. *Frontiers in microbiology* **2016,** *7*, 529-529.
16. Rai, A. N.; Singh, A. K.; Syiem, M. B., Chapter 23 - Plant Growth-Promoting Abilities in Cyanobacteria. In *Cyanobacteria*, Mishra, A. K.; Tiwari, D. N.; Rai, A. N., Eds. Academic Press: 2019; pp 459-476.
17. Wang, J.; Koo, Y.; Alexander, A.; Yang, Y.; Westerhof, S.; Zhang, Q.; Schnoor, J. L.; Colvin, V. L.; Braam, J.; Alvarez, P. J. J., Phytostimulation of Poplars and Arabidopsis Exposed to Silver Nanoparticles and Ag+ at Sublethal Concentrations. *Environmental Science & Technology* **2013,** *47* (10), 5442-5449.
18. Zhang, H.; Du, W.; Peralta-Videa, J. R.; Gardea-Torresdey, J. L.; White, J. C.; Keller, A.; Guo, H.; Ji, R.; Zhao, L., Metabolomics Reveals How Cucumber (Cucumis sativus) Reprograms Metabolites To Cope with Silver Ions and Silver Nanoparticle-Induced Oxidative Stress. *Environmental Science & Technology* **2018,** *52* (14), 8016-8026.
19. Wu, D.; Yang, S.; Du, W.; Yin, Y.; Zhang, J.; Guo, H., Effects of titanium dioxide nanoparticles on Microcystis aeruginosa and microcystins production and release. *Journal of Hazardous Materials* **2019,** *377*, 1-7.
20. Sigalat, C.; de Kouchkowski, Y., Fractionnement et caracterisation de l'algue bleue unicellulaire Anacystis nidulans. *Physiol Veg* **1975,** 13, 243–258.
21. Belnap, J., Nitrogen fixation in biological soil crusts from southeast Utah, USA. *Biology and Fertility of Soils* **2002,** *35* (2), 128-135.
22. Wang, X.; Teng, Y.; Tu, C.; Luo, Y.; Greening, C.; Zhang, N.; Dai, S.; Ren, W.; Zhao, L.; Li, Z., Coupling between Nitrogen Fixation and Tetrachlorobiphenyl Dechlorination in a Rhizobium–Legume Symbiosis. *Environmental Science & Technology* **2018,** *52* (4), 2217-2224.
23. Studt, J. L.; Campbell, E. R.; Westrick, D.; Kinnunen-Skidmore, T.; Marceau, A. H.; Campbell, W. H., Non-toxic total nitrogen determination using a low alkaline persulfate digestion. *MethodsX* **2020,** *7*, 100791.

24. Zhang, M.; Wang, H.; Liu, P.; Song, Y.; Huang, H.; Shao, M.; Liu, Y.; Li, H.; Kang, Z., Biotoxicity of degradable carbon dots towards microalgae Chlorella vulgaris. *Environmental Science: Nano* **2019,** *6* (11), 3316-3323.
25. Jambunathan, N., Determination and Detection of Reactive Oxygen Species (ROS), Lipid Peroxidation, and Electrolyte Leakage in Plants. In *Plant Stress Tolerance: Methods and Protocols*, Sunkar, R., Ed. Humana Press: Totowa, NJ, 2010; pp 291-297.
26. Schwarz, D.; Nodop, A.; Hüge, J.; Purfürst, S.; Forchhammer, K.; Michel, K.-P.; Bauwe, H.; Kopka, J.; Hagemann, M., Metabolic and Transcriptomic Phenotyping of Inorganic Carbon Acclimation in the Cyanobacterium Synechococcus elongatus PCC 7942. *Plant Physiology* **2011,** *155* (4), 1640-1655.
27. Xia, J.; Sinelnikov, I. V.; Han, B.; Wishart, D. S., MetaboAnalyst 3.0—making metabolomics more meaningful. *Nucleic Acids Res.* **2015,** *43* (W1), W251-W257.
28. Jung, Y.; Ahn, Y. G.; Kim, H. K.; Moon, B. C.; Lee, A. Y.; Hwang, G.-S., Characterization of dandelion species using 1H NMR-and GC-MS-based metabolite profiling. *Analyst* **2011,** *136* (20), 4222-4231.
29. Xia, J.; Wishart, D. S., MSEA: a web-based tool to identify biologically meaningful patterns in quantitative metabolomic data. *Nucleic Acids Res.* **2010,** *38* (suppl 2), W71-W77.
30. Jarvie, H. P.; Al-Obaidi, H.; King, S. M.; Bowes, M. J.; Lawrence, M. J.; Drake, A. F.; Green, M. A.; Dobson, P. J., Fate of silica nanoparticles in simulated primary wastewater treatment. *Environ. Sci. Technol.* **2009,** *43*, 8622.
31. Batley, G. E.; Kirby, J. K.; McLaughlin, M. J., Fate and Risks of Nanomaterials in Aquatic and Terrestrial Environments. *Accounts of Chemical Research* **2013,** *46* (3), 854-862.
32. von Moos, N.; Bowen, P.; Slaveykova, V. I., Bioavailability of inorganic nanoparticles to planktonic bacteria and aquatic microalgae in freshwater. *Environmental Science: Nano* **2014,** *1* (3), 214-232.
33. Handy, R. D.; Owen, R.; Valsami-Jones, E., The ecotoxicology of nanoparticles and nanomaterials: current status, knowledge gaps, challenges, and future needs. *Ecotoxicology* **2008,** *17* (5), 315-325.
34. Ma, S.; Lin, D., The biophysicochemical interactions at the interfaces between nanoparticles and aquatic organisms: adsorption and internalization. *Environmental Science: Processes & Impacts* **2013,** *15* (1), 145-160.
35. Zhang, L.; Lei, C.; Yang, K.; White, J. C.; Lin, D., Cellular response of Chlorella pyrenoidosa to oxidized multi-walled carbon nanotubes. *Environmental Science: Nano* **2018,** *5* (10), 2415-2425.
36. Duong, T. T.; Le, T. S.; Tran, T. T. H.; Nguyen, T. K.; Ho, C. T.; Dao, T. H.; Le, T. P. Q.; Nguyen, H. C.; Dang, D. K.; Le, T. T. H.; Ha, P. T., Inhibition effect of engineered silver nanoparticles to bloom forming cyanobacteria. *Advances in Natural Sciences: Nanoscience and Nanotechnology* **2016,** *7* (3).
37. Köser, J.; Engelke, M.; Hoppe, M.; Nogowski, A.; Filser, J.; Thöming, J., Predictability of silver nanoparticle speciation and toxicity in ecotoxicological media. *Environmental Science: Nano* **2017,** *4* (7), 1470-1483.
38. Nel, A.; Xia, T.; Mädler, L.; Li, N., Toxic Potential of Materials at the Nanolevel. *Science* **2006,** *311* (5761), 622-627.

39. Alberte, R. S.; Tel-Or, E.; Packer, L.; Thornber, J. P., Functional organisation of the photo-synthetic apparatus in heterocysts of nitrogen-fixing cyanobacteria. *Nature* **1980,** *284* (5755), 481-483.
40. He, D.; Dorantes-Aranda, J. J.; Waite, T. D., Silver Nanoparticle—Algae Interactions: Oxidative Dissolution, Reactive Oxygen Species Generation and Synergistic Toxic Effects. *Environmental Science & Technology* **2012,** *46* (16), 8731-8738.
41. Axelsen, P. H.; Komatsu, H.; Murray, I. V. J., Oxidative Stress and Cell Membranes in the Pathogenesis of Alzheimer's Disease. *Physiology* **2011,** *26* (1), 54-69.
42. Mandal, S. M.; Chakraborty, D.; Dey, S., Phenolic acids act as signaling molecules in plant-microbe symbioses. *Plant signaling & behavior* **2010,** *5*, 359-68.
43. Cessna, S.; Sears, V.; Dickman, M.; Low, P., Oxalic Acid, a Pathogenicity Factor for Sclerotinia sclerotiorum, Suppresses the Oxidative Burst of the Host Plant. *The Plant cell* **2000,** *12*, 2191-200.
44. Kim, E. J.; Baik, E.; Jung, S.; Won, R.; Nahm, T.; Lee, B., Dehydroascorbic acid prevents oxidative cell death through a glutathione pathway in primary astrocytes. *Journal of neuroscience research* **2005,** *79*, 670-9.
45. Dubreuil, C.; Poinssot, B., Role of glutathione in plant signaling under biotic stress. *Plant signaling & behavior* **2012,** *7*, 210-2.

Figure legends

Figure 1. SEM images of cyanobacteria exposed to different concentrations of AgNPs (**A1** control without AgNPs, **A2** 0.1 mg/L, **A3** 1 mg/L). EDS detected the elemental distribution of Ag in cyanobacteria (**B1** control without AgNPs, **B2** 0.1 mg/L, **B3** 1 mg/L). Cyanobacteria are cultivated with AgNPs for 96 h at 25 ºC with the light intensity of 36 μmol photons m^{-2} s^{-1}.

Figure 2. Biomass of cyanobacteria reflected by optical density at 680 nm. Cyanobacteria are exposed to AgNPs (**A**) and Ag^+ (**B**); Chlorophyll content of cyanobacteria treated with AgNPs (**C**) and Ag^+ (**D**). Visual comparison of cyanobacteria exposed to different concentrations of AgNPs (**E**) and Ag^+ (**F**). Cyanobacteria cells are cultivated with AgNPs for 96 h at 25 ºC with the light intensity of 36 μmol photons m^{-2} s^{-1}. AgNPs: 0, 0.01, 0.1, 1 mg/L; Ag^+: 0, 0.1, 1, 10 μg/L. Error bars represent standard deviations (n = 4). Lowercase letters indicate significant differences between treatments.

Figure 3. Nitrogenase activity of cyanobacteria treated with AgNPs (**A**) and Ag^+ (**B**). Total nitrogen content of cyanobacteria treated with AgNPs (**C**) and Ag^+ (**D**). Cyanobacteria cells are cultivated with AgNPs for 96 h at 25 ºC with the light intensity of 36 μmol photons m^{-2} s^{-1}. AgNPs: 0, 0.01, 0.1, 1 mg/L; Ag^+: 0, 0.1, 1, 10 μg/L. Error bars represent standard deviations (n = 4). Lowercase letters indicate significant differences between treatments.

Figure 4. ROS content of cyanobacteria treated with AgNPs (**A**) and Ag^+ (**B**). MDA content of cyanobacteria treated with AgNPs (**C**) and Ag^+ (**D**), respectively. Cyanobacteria cells are cultivated with AgNPs for 96 h at 25 ºC with the light intensity of

36 μmol photons m^{-2} s^{-1}. AgNPs: 0, 0.01, 0.1, 1 mg/L; Ag^{+}: 0, 0.1, 1, 10 μg/L. Error bars represent standard deviations (n = 4). Lowercase letters indicate significant differences between treatments.

Figure 5. Partial leas-squares discriminate analysis (PLS-DA) score plots of metabolic profiles in cyanobacteria treated with AgNPs (**A**) and Ag^{+} (**B**); (**C**) Venn diagram of significantly changed metabolites in cyanobacteria treated with AgNPs and Ag^{+}. AgNPs: 0, 0.01, 0.1, 1 mg/L; Ag^{+}: 0, 0.1, 1, 10 μg/L.

Figure 6. Box plots of relative abundance of antioxidant metabolites in cyanobacteria exposed to different doses of AgNPs and Ag^{+} (n = 4). A−D represent 0, 0.01, 0.1, 1 mg/L AgNPs, respectively; E-G represent 0.1, 1, 10 μg/L Ag^{+}, respectively.

Figure 7. Box plots of relative abundance of oxalic acid in cyanobacteria treated with different doses of AgNPs and Ag^{+} (n = 4). A−D represent 0, 0.01, 0.1, 1 mg/L AgNPs, respectively; E-G represent 0.1, 1, 10 μg/L Ag^{+}, respectively.

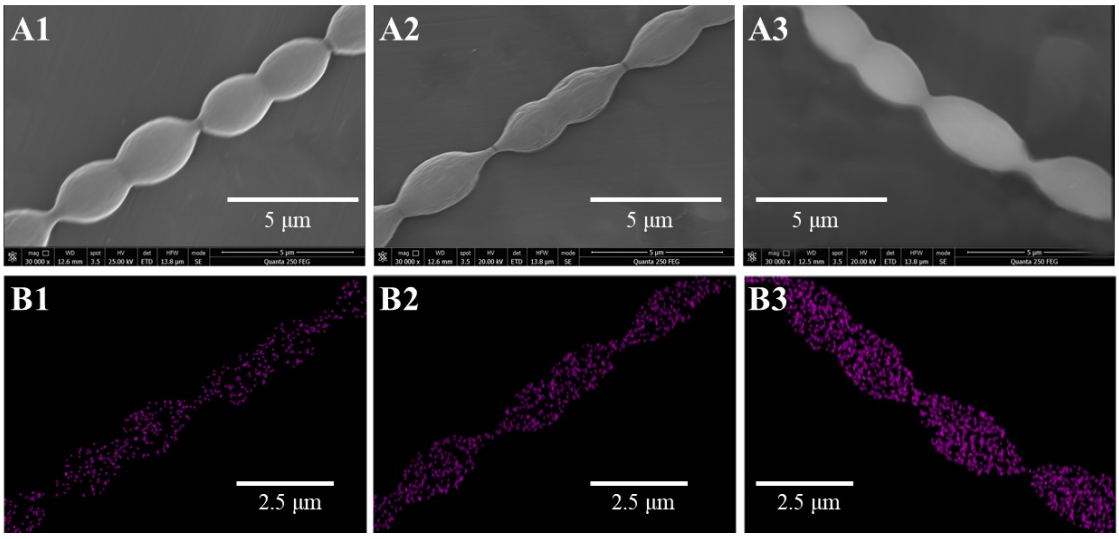

Figure 1.

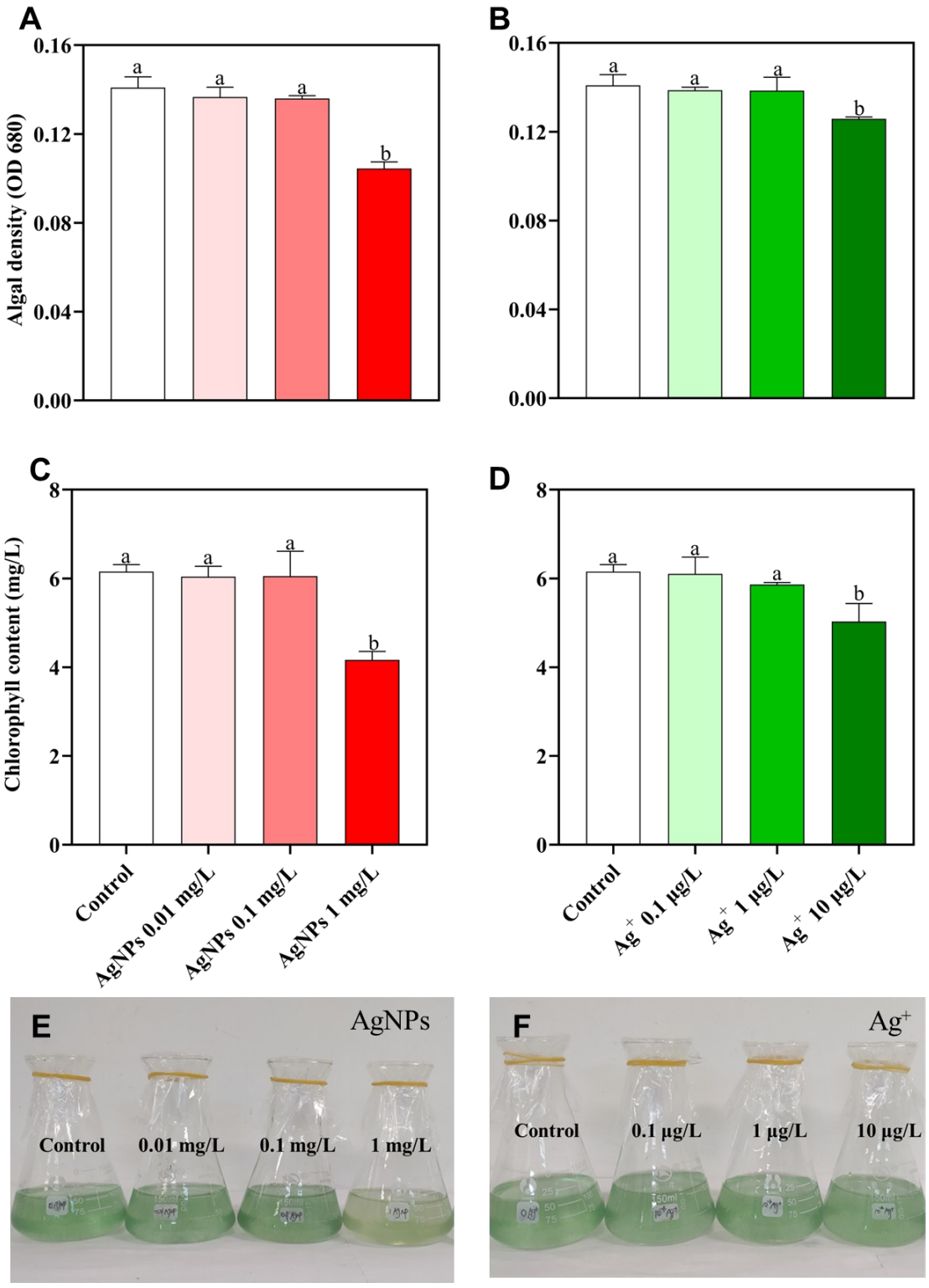
A
B
C
D
Algal density (OD 680)
Chlorophyll content (mg/L)
0.16
0.12
0.08
0.04
0.00
8
6
4
2
0
a
b
Control
AgNPs 0.01 mg/L
AgNPs 0.1 mg/L
AgNPs 1 mg/L
Ag+ 0.1 µg/L
Ag+ 1 µg/L
Ag+ 10 µg/L
E
AgNPs
Control
0.01 mg/L
0.1 mg/L
1 mg/L
F
Ag+
Control
0.1 µg/L
1 µg/L
10 µg/L

Figure 2.

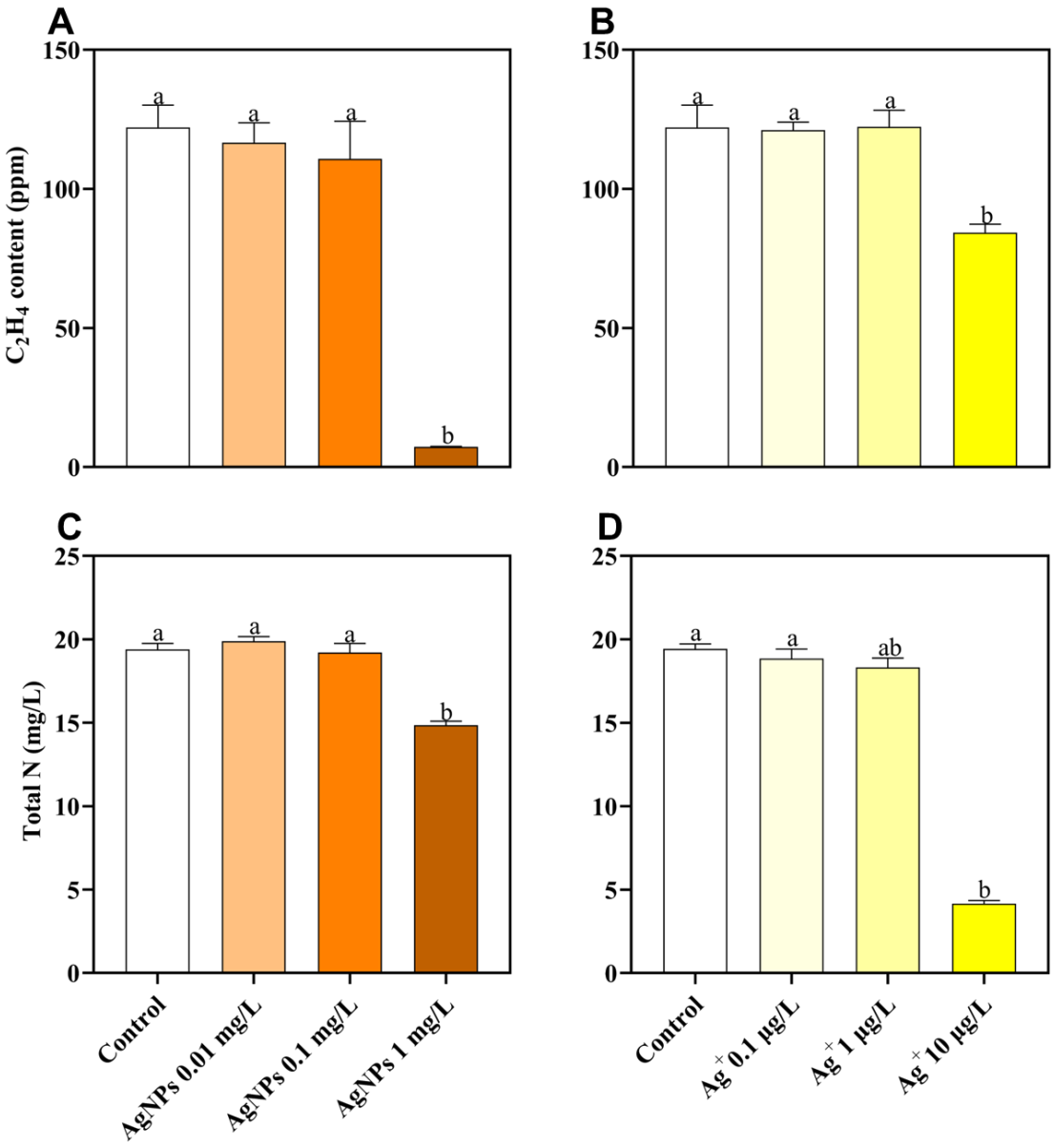
A
B
C
D
C_2H_4 content (ppm)
Total N (mg/L)
150
100
50
0
25
20
15
10
5
a
ab
b
Control
AgNPs 0.01 mg/L
AgNPs 0.1 mg/L
AgNPs 1 mg/L
Ag+ 0.1 µg/L
Ag+ 1 µg/L
Ag+ 10 µg/L

Figure 3.

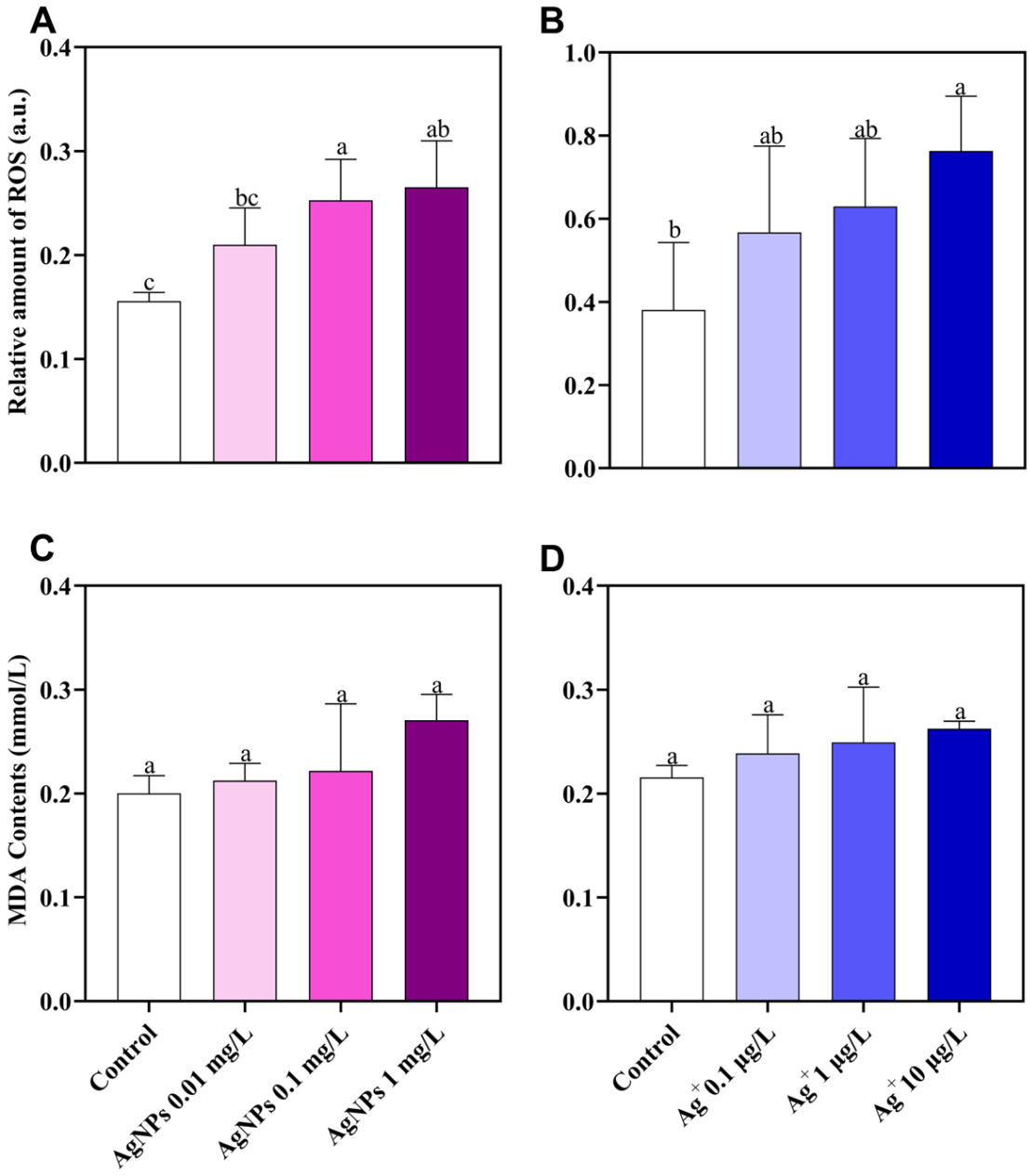
A
B
C
D
Relative amount of ROS (a.u.)
MDA Contents (mmol/L)
0.0
0.1
0.2
0.3
0.4
0.6
0.8
1.0
c
bc
a
ab
b
ab
ab
a
a
a
a
a
a
a
a
a
Control
AgNPs 0.01 mg/L
AgNPs 0.1 mg/L
AgNPs 1 mg/L
Control
Ag+ 0.1 µg/L
Ag+ 1 µg/L
Ag+ 10 µg/L

Figure 4.

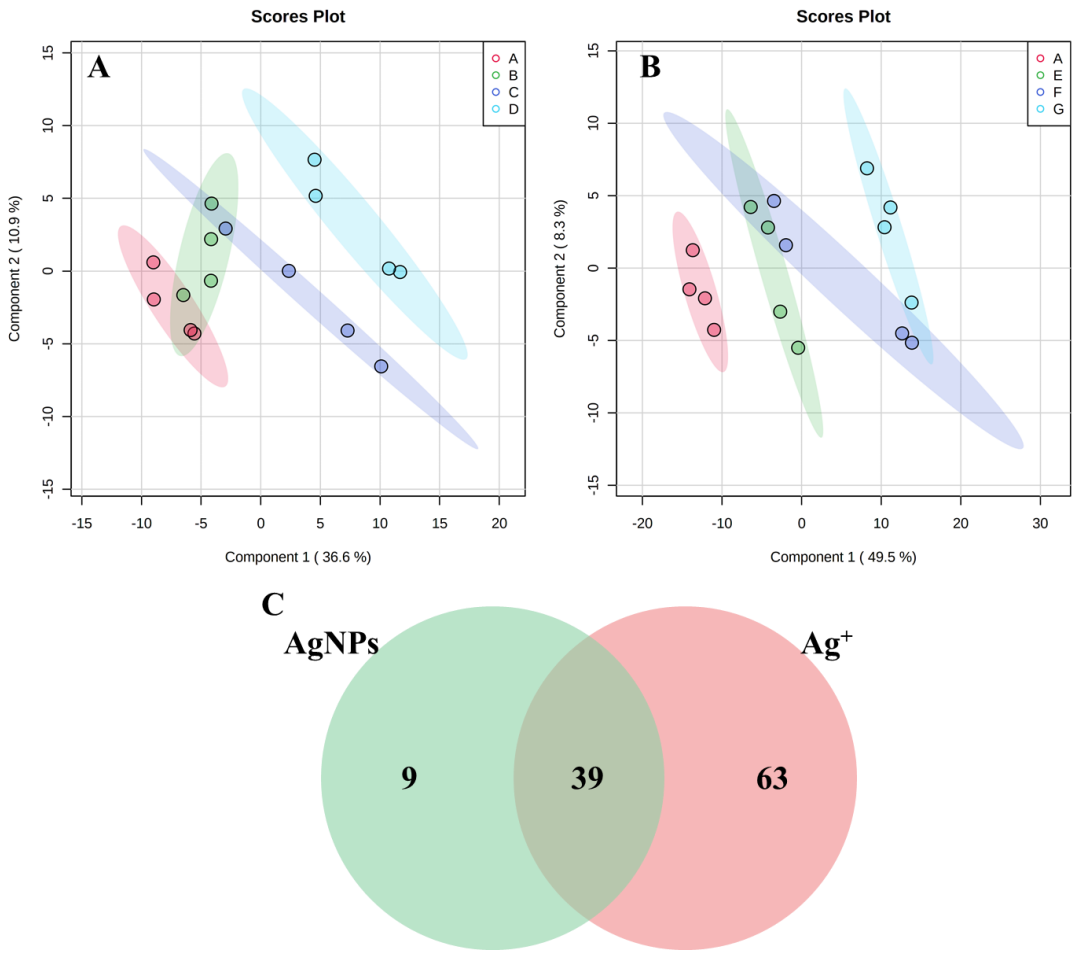
Scores Plot
A
A
B
C
D
Component 2 (10.9 %)
Component 1 (36.6 %)
Scores Plot
B
A
E
F
G
Component 2 (8.3 %)
Component 1 (49.5 %)
C
AgNPs
Ag+
9
39
63

Figure 5.

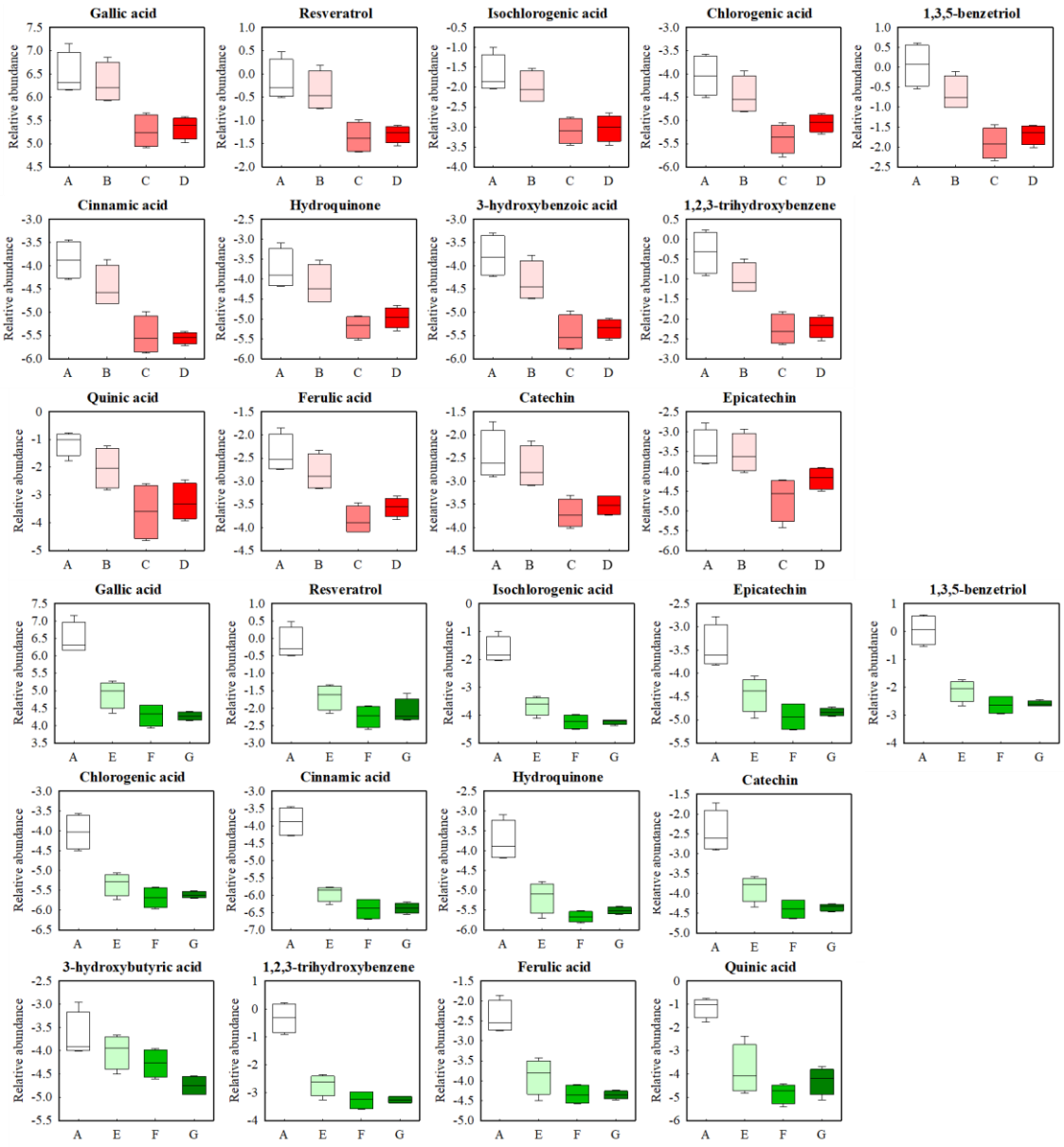
Gallic acid
Resveratrol
Isochlorogenic acid
Chlorogenic acid
1,3,5-benzetriol
Cinnamic acid
Hydroquinone
3-hydroxybenzoic acid
1,2,3-trihydroxybenzene
Quinic acid
Ferulic acid
Catechin
Epicatechin
Gallic acid
Resveratrol
Isochlorogenic acid
Epicatechin
1,3,5-benzetriol
Chlorogenic acid
Cinnamic acid
Hydroquinone
Catechin
3-hydroxybutyric acid
1,2,3-trihydroxybenzene
Ferulic acid
Quinic acid
Relative abundance
A B C D
A E F G

Figure 6.

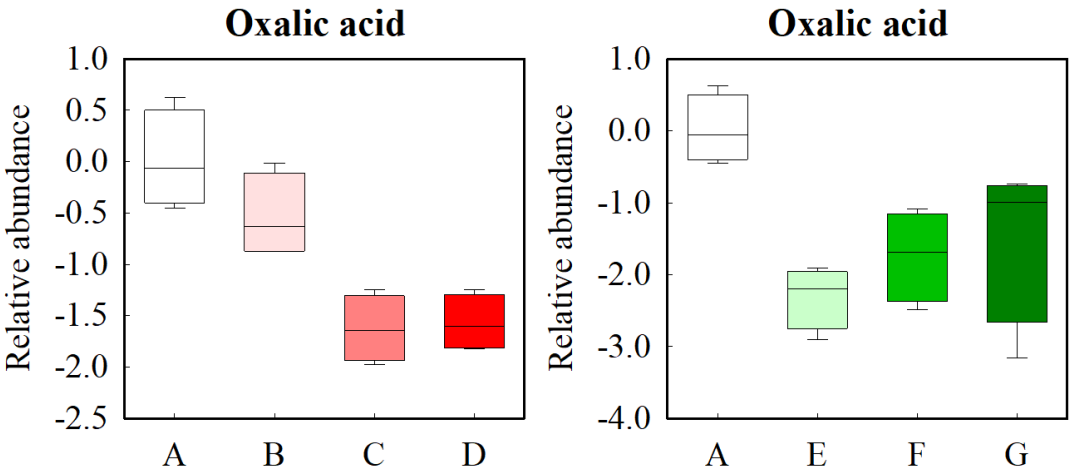
Oxalic acid
Relative abundance
1.0
0.5
0.0
-0.5
-1.0
-1.5
-2.0
-2.5
A
B
C
D
Oxalic acid
Relative abundance
1.0
0.0
-1.0
-2.0
-3.0
-4.0
A
E
F
G

Figure 7.